

# HYBRIDISATION OF CFRP WITH CONTINUOUS METAL FIBRES FOR DAMAGE TOLERANT AND HIGHLY CONDUCTIVE LIGHTWEIGHT STRUCTURES

Benedikt Hannemann<sup>1</sup>, Sebastian Backe<sup>2</sup>, Sebastian Schmeer<sup>1</sup>, Frank Balle<sup>2</sup>, Ulf P. Breuer<sup>1</sup>

<sup>1</sup> Institute for Composite Materials (IVW GmbH), Erwin-Schroedinger-Str., Building 58, 67663  
Kaiserslautern, Germany, [benedikt.hannemann@ivw.uni-kl.de](mailto:benedikt.hannemann@ivw.uni-kl.de), [www.ivw.uni-kl.de](http://www.ivw.uni-kl.de)

<sup>2</sup> Institute of Materials Science and Engineering (WKK), University of Kaiserslautern, P.O. Box 3049,  
67653 Kaiserslautern, Germany, [sbacke@mv.uni-kl.de](mailto:sbacke@mv.uni-kl.de), [www.mv.uni-kl.de/wkk](http://www.mv.uni-kl.de/wkk)

**Keywords:** Damage tolerance, Electrical conductivity, Hybrid composite, Multifunctionality

## ABSTRACT

Carbon fibre reinforced polymers (CFRP) offer superior weight-specific mechanical properties. However, their brittle failure behaviour limits the structural integrity and damage tolerance in case of impact and crash events. Furthermore, the electrical conductivity is insufficient for certain applications (e.g. lightning strike protection, signal transfer, grounding). Former research attempts tried to resolve these deficits by modifying the resin system, but could not prove sufficient enhancements. A novel approach is the incorporation of highly conductive and ductile endless metal fibres into the CFRP, thus merging electrical and load-bearing functions within the metal fibres. In this context, the present study focuses on optimising the structural and electrical performance of such hybrid composites with shares of metal fibres up to 20 vol.%. Researches are carried out on unidirectional and multiaxial laminates. Synchronous improvements of the electrical conductivity, the impact and penetration resistance, the notched properties as well as the energy absorption can be verified. Additionally, the application of integrated metastable metal fibres for in-situ and post-damage health monitoring by measurement of deformation induced-phase transformations is proved.

## 1 INTRODUCTION

Despite increasing requirements by customers, operators and authorities, the weight of aircrafts primary structure could continuously be decreased to today's level of approximately 25 kg per passenger and 1 000 km of range [1]. The necessary weight reduction has been achieved by improved load prediction, new design principles, improved design and sizing methods, improved manufacturing processes and application of enhanced materials. In this context, artificial composite materials, especially carbon fibre reinforced polymers (CFRP) have been continuously and progressively introduced to aeronautics over the past decades. CFRP offers superior weight-specific mechanical properties, excellent fatigue behaviour, pronounced media and corrosion resistance.

However, the lightweight potential of CFRP over modern aluminium alloys is still severely limited due its relatively poor electrical conductivity. Additional metal components are necessary to provide electrical functionality to the airframe structure, such as expended copper foils on the outer skin for lightning strike protection, wires for electrical bonding and grounding or overbraiding of cables to provide sufficient shielding. Former research attempts tried to address these issues by modifying the polymer matrix system, e.g. by introduction of conductive particles like carbon nano tubes (CNT) [2], [3]. However, a sufficient level of conductivity which would guarantee electrical function integration for the modified CFRP similar to that of aluminium alloys or glass fibre reinforced metal laminates (GLARE) could not be demonstrated. Moreover, the brittle failure behaviour of CFRP limits the damage tolerance and structural integrity in case of impact (e.g. tool drop, bird strike, hail strike, ramp collision) and crash events. To ensure the necessary robustness, a minimum skin thickness is therefore prescribed for the fuselage, partially exceeding stiffness and strength requirements. A minimum skin thickness is also necessary to ensure state-of-the-art bolted repair technologies. The impact damage tolerance of thin-walled CFRP structures has gradually been improved by the addition of polymer

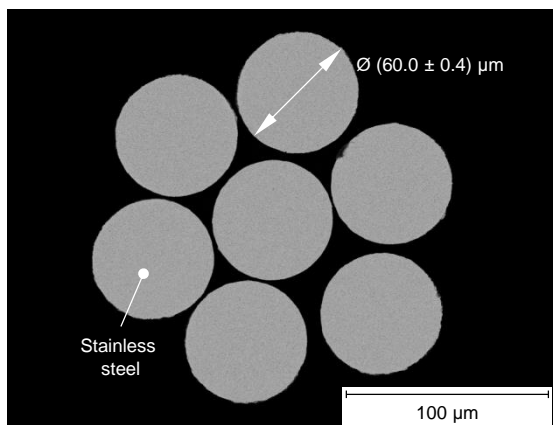
toughening agents [4], [5]. Thermoplastic polymers and rubber particles were introduced in epoxy resin systems, enabling substantial improvements of fracture toughness and residual strength. However, the minimum skin thickness criterion can still be the limiting design driver. A reduction of this value requires material enhancements in terms of damage tolerance against impact and improved head pull-through resistance.

## 2 FIBRE HYBRID LAMINATES

In this context, a hybrid composite consisting of continuous carbon and metal reinforcement fibres embedded in an epoxy matrix is investigated. Basic idea of this novel material concept is to merge electrical and load-bearing functions by incorporated highly conductive and ductile metal fibres. The increased density of the composite is over-compensated by eliminating the need for additional electrical system installation items and the enhanced damage tolerance, resulting in a reduced minimum skin thickness. The integrated metal fibres can either be distributed homogenously in the entire composite (“homogenised layer concept”) or locally concentrated in individual layers (“separated layer concept”). The fibre based approach enables utilisation of anisotropy for stress tailored composite design and wrinkle-free fabrication of multiple shaped structures. Moreover, fully automated manufacturing technologies that are already available and in service for CFRP can be explored, e.g. automated tape laying, fibre placement or resin transfer moulding.

For the selection of potential metal fibres various requirements have to be considered, in particular superior electrical conductivity, distinctive failure strain, high strength, high stiffness, corrosion resistance, appropriate thermal expansion, availability and low costs. Stainless steel fibres are commercially available with a wide range of mechanical properties and appearance. The stiffness of standard modulus carbon and stainless steel fibres is comparable. Compared to a standard high tenacity ex-PAN carbon fibre, the electrical conductance of stainless steel fibres is approximately 23 times higher. Due to less alloying, low carbon steel fibres have even better specific mechanical properties. By nickel or copper cladding, the electrical conductivity can be further enhanced. In addition, the cladding enables a sufficient corrosion resistance.

Within the present study, twisted bundles of metastable austenitic stainless steel fibres are used. The bundle consists of seven filaments, each with a diameter of 60  $\mu\text{m}$ . Furthermore, standard modulus/high tenacity carbon fibres of type Toho Tenax HTS40 and epoxy resin of type Cytec CYCOM 977-2 are processed. Selected properties of the fibres are summarised in figure 1 [6].



|                                        | Carbon fibre <sup>1)</sup> | Steel fibre <sup>2)</sup>        |
|----------------------------------------|----------------------------|----------------------------------|
| Density / g/cm <sup>3</sup>            | 1.77                       | 7.95 ± 0.01                      |
| Young's modulus / GPa                  | 240                        | 177 ± 7                          |
| Tensile strength / MPa                 | 4 300                      | 897 ± 2                          |
| Failure strain / %                     | 1.80                       | 32.31 ± 2.01                     |
| Electr. resistivity / $\Omega\text{m}$ | $1.6 \times 10^{-5}$       | $(6.97 \pm 0.02) \times 10^{-7}$ |
| Filament diameter / $\mu\text{m}$      | 5                          | 60.0 ± 0.4                       |
| Filaments per roving                   | 12k                        | 7                                |

<sup>1)</sup> Manufacturer information <sup>2)</sup> Own measurements on fibre bundles

Figure 1: Selected properties of processed carbon and metal fibres

## 3 RESEARCHES ON UNIAXIAL LAYERS

In a first step, the mechanical properties of unidirectional (UD) reinforced laminates are analysed. Hybrid composites with volume shares of 10.4 % (SCFRP 10) and 18.8 % (SCFRP 20) of steel fibres are tested and compared with state-of-the-art CFRP and pure SFRP. Detailed information on the tested laminates and the obtained test results are given in [1] and [7].

### 3.1 Plain tension tests

In case of pure tensile load in parallel to the fibre orientation, both CFRP and the hybrid composites show brittle material behaviour with similar ultimate strains to failure. Increasing the steel fibre content lowers the tensile strength and stiffness of the composite. Despite the integration of highly ductile metal fibres, a pseudo-ductile behaviour after failure initiation cannot be observed. This brittleness of the hybrid composites is caused by homogenous load state within the specimen. When loading the specimen, both the carbon and steel fibres elongate elastically on the entire gauge length, thus generate elastic energy. During failure of the carbon fibres, the elastic energy is abruptly released and transferred to the steel fibres, causing pronounced yielding of the metal. However, the steel fibres yield only in a narrow area around the fracture, causing merely a slight macroscopic elongation of the specimen. In large areas of the specimen, the available ductility of the metal fibres is far from being exhausted. Improvements are expected by higher steel fibre fractions (i.e. elastic energy can be absorbed by an increased amount of steel fibres), but would cause higher material densities. Furthermore, a reduced metal fibre-resin-adhesion could enable unhindered deformation of the metal fibres at larger areas, but would certainly impact other important properties, e.g. transverse tensile strength. In addition, the amount of released elastic energy can be reduced by multiaxial stacking sequences.

### 3.2 Electrical conductivity tests

Electrical conductivity measurements in parallel to the fibre orientation are examined by the two-wire-method. The conductivity measurements verify a correlation of the volume conductivity of the composite with the volume share and the specific electrical resistance of the incorporated metal fibres. Compared to CFRP, the electrical conductivity of the hybrid composites is about three times higher for a steel fibre fraction of 10.4 vol.% and five times higher for steel fibre fraction of 18.8 vol.%. Further enhancements are feasible with higher steel fibre percentages. The analysis, however, also discloses the challenge of establishing a sufficient connection to the hybrid composites in order to exploit their inherently given electrical conductivity.

## 4 RESEARCHES ON MULTIAXIAL LAMINATES

As reference materials, 13- and 17-layered CFRP laminates with typical aeronautical stacking sequences are manufactured. For benchmark reasons, a 13-layered CFRP laminate with an additional copper mesh for lightning strike protection purposes (Dexmet 3CU7-100FA, 195 g/m<sup>2</sup>) is prepared. The hybrid composites consist of a 13-layered CFRP core and two or four additional, pure steel fibre reinforced layers, table 1. The laminates are tested with regard to their post-failure behaviour, their notched properties and their impact performance.

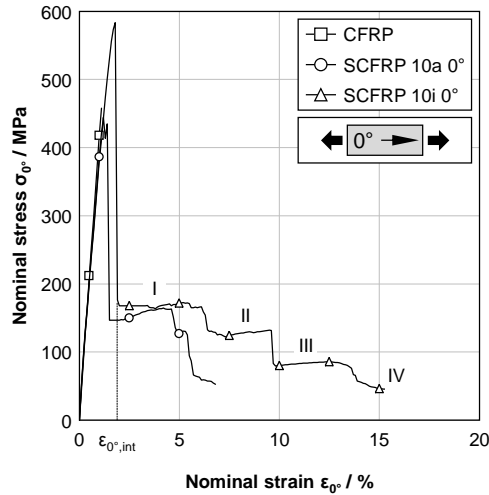
Table 1: Microstructure of the analysed multiaxial laminates

| Laminate          | Stacking sequence <sup>1)</sup>                                                                                                                                         | $\Phi_{\text{Carbon}} / \text{vol.}\%$ <sup>2)</sup> | $\Phi_{\text{Steel}} / \text{vol.}\%$ <sup>2)</sup> | $\Phi_{\text{Resin}} / \text{vol.}\%$ <sup>2)</sup> | t / mm <sup>3)</sup> | $\rho / \text{g/cm}^3$ <sup>4)</sup> |
|-------------------|-------------------------------------------------------------------------------------------------------------------------------------------------------------------------|------------------------------------------------------|-----------------------------------------------------|-----------------------------------------------------|----------------------|--------------------------------------|
| (1) CFRP          | (45 <sup>c</sup> /-45 <sup>c</sup> /45 <sup>c</sup> /-45 <sup>c</sup> /90 <sup>c</sup> /0 <sup>c</sup> /90 <sup>c</sup> ) <sub>s</sub>                                  | 61.6                                                 | 0.0                                                 | 38.4                                                | 1.60                 | 1.59                                 |
| (2) CFRP thick    | (0 <sup>c</sup> /90 <sup>c</sup> /45 <sup>c</sup> /-45 <sup>c</sup> /45 <sup>c</sup> /-45 <sup>c</sup> /90 <sup>c</sup> /0 <sup>c</sup> /90 <sup>c</sup> ) <sub>s</sub> | 60.7                                                 | 0.0                                                 | 39.3                                                | 2.12                 | 1.59                                 |
| (3) CFRP + Cu     | (0 <sup>c</sup> /45 <sup>c</sup> /-45 <sup>c</sup> /45 <sup>c</sup> /-45 <sup>c</sup> /90 <sup>c</sup> /0 <sup>c</sup> /90 <sup>c</sup> ) <sub>s</sub>                  | 58.5                                                 | 0.0                                                 | 40.2                                                | 1.68                 | 1.68                                 |
| (4) SCFRP 10a 0°  | (0 <sup>s</sup> /45 <sup>c</sup> /-45 <sup>c</sup> /45 <sup>c</sup> /-45 <sup>c</sup> /90 <sup>c</sup> /0 <sup>c</sup> /90 <sup>c</sup> ) <sub>s</sub>                  | 52.7                                                 | 11.2                                                | 36.2                                                | 1.87                 | 2.29                                 |
| (5) SCFRP 10a 90° | (90 <sup>s</sup> /45 <sup>c</sup> /-45 <sup>c</sup> /45 <sup>c</sup> /-45 <sup>c</sup> /90 <sup>c</sup> /0 <sup>c</sup> /90 <sup>c</sup> ) <sub>s</sub>                 | 52.7                                                 | 11.2                                                | 36.2                                                | 1.87                 | 2.29                                 |
| (6) SCFRP 10i 0°  | (0 <sup>c</sup> /45 <sup>c</sup> /-45 <sup>c</sup> /45 <sup>c</sup> /-45 <sup>c</sup> /90 <sup>c</sup> /0 <sup>s</sup> /90 <sup>c</sup> ) <sub>s</sub>                  | 52.7                                                 | 11.2                                                | 36.2                                                | 1.87                 | 2.29                                 |
| (7) SCFRP 20a     | (0 <sup>s</sup> /90 <sup>s</sup> /45 <sup>c</sup> /-45 <sup>c</sup> /45 <sup>c</sup> /-45 <sup>c</sup> /90 <sup>c</sup> /0 <sup>c</sup> /90 <sup>c</sup> ) <sub>s</sub> | 46.0                                                 | 19.5                                                | 34.5                                                | 2.14                 | 2.82                                 |

<sup>1)</sup> C: Carbon fibre, S: Steel fibre, Cu: Copper mesh <sup>2)</sup> Volume share <sup>3)</sup> Laminate thickness <sup>4)</sup> Density

#### 4.1 Plain tension tests

Monotonic tensile tests are conducted in compliance with DIN EN ISO 527-4. Rectangular specimens with a width of 25 mm are monotonically loaded with a crosshead speed of 2 mm/min. The elongation of the specimen is analysed within a gauge length of 150 mm by a DIC (digital image correlation) system. For each tested material configuration, five specimens are tested to failure. The obtained results are shown in figure 2.



| Material     | $\sigma_{0^\circ, \max} / \text{MPa}$ | $\epsilon_{0^\circ, \text{int}} / \%$ | $\epsilon_{0^\circ, \max} / \%$ |
|--------------|---------------------------------------|---------------------------------------|---------------------------------|
| CFRP         | $510 \pm 19$                          | $1.23 \pm 0.06$                       | $1.23 \pm 0.06$                 |
| SCFRP 10a 0° | $457 \pm 6$                           | $1.22 \pm 0.05$                       | $7.66 \pm 1.49$                 |
| SCFRP 10i 0° | $597 \pm 13$                          | $1.87 \pm 0.03$                       | $11.77 \pm 4.95$                |

<sup>1)</sup> Nominal total strain in 0° at failure initiation

Figure 2: Results of quasi-static plain tension tests on multiaxial (hybrid) laminates

CFRP shows a linear elastic behaviour with brittle failure. Failure occurs singularly at a nominal strain of 1.23 %. By contrast, both hybrid composites SCFRP 10i 0° and SCFRP 10a 0° with two inner or two outer steel fibre reinforced layers exhibit a pronounced post-failure behaviour. In case of SCFRP 10i 0° failure is initiated at a nominal total strain of 1.87 %. However, different to the UD laminates, less elastic energy is released from the CFRP core at this moment due to its multiaxial stacking sequence. The available ductility of the steel fibres is not exhausted by the corresponding energy transfer. As a consequence, the steel fibres can bear further elongation. Compared to CFRP, the ultimate strain to failure is 10 times higher. After final failure of the carbon fibres, four different stress levels can be differed. Both lower stress levels (cf. figure 2, III + IV) correspond to yielding of the steel fibre reinforced layers. The upper levels relate to deformations of the  $\pm 45^\circ$ -CFRP-layers (I + II): Due to the energy absorption capability of the steel fibre plies, the  $\pm 45^\circ$ -CFRP-layers are not completely damaged by the energy release during failure of the 0°-CFRP-Layers. Furthermore, the intact steel fibre plies bypass inter-laminar failure within the  $\pm 45^\circ$ -CFRP-plies and activate intact carbon fibres. Consequently, the hybrid material behaviour under load is not only a superimposition of the stress-strain behaviours of CFRP and pure SFRP, but a complex interaction. SCFRP 10a 0° exhibits a similar stress-strain-behaviour as SCFRP 10i 0°. However, the steel fibre reinforced top layers act as a protective cover. The elastic energy release of the carbon fibres blasts the entire laminate and causes a pre-damage of the steel fibre plies. This is different to SCFRP 10i 0°, where the laminate can burst to both sides of the composite, consequently without less severe influence on the inner steel fibre plies. As a consequence, the strain at initial failure (1.22 %), the maximum strength (457 MPa) and the ultimate elongation (7.66 %) are lower, compared to SCFRP 10i 0°.

#### 4.2 Dynamic bearing stress tests

A metal pin with a diameter of 6.35 mm is continuously pulled in in-plane direction through plain specimens with a loading speed of 1 m/s. In order to clearly assess the influence of the steel fibre reinforcement on the bearing behaviour, only hybrid composites with steel fibres either in parallel (SCFRP 10a 0°) or transverse (SCFRP 10a 90°) to the pin motion are investigated and compared with CFRP and CFRP + Cu. For each laminate configuration, five specimens are analysed. All tested laminate configurations show a similar material response: after exceeding an initial trigger load ( $F_{\text{trig}}$ )

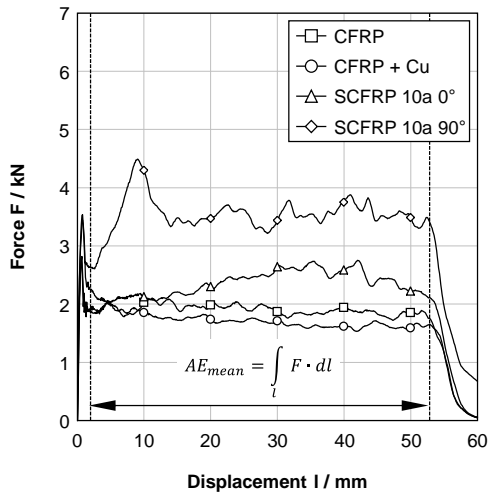


Figure 3: Results of dynamic shear-out tests on multiaxial (hybrid) laminates

| Material      | $F_{trig} / N$ | $F_{mean} / N$ <sup>1)</sup> | $AE_{mean} / J$ <sup>1)</sup> |
|---------------|----------------|------------------------------|-------------------------------|
| CFRP          | 2 903 ± 183    | 1 902 ± 80                   | 97 ± 4                        |
| CFRP + Cu     | 2 810 ± 191    | 1 713 ± 237                  | 87 ± 12                       |
| SCFRP 10a 0°  | 3 587 ± 303    | 2 358 ± 171                  | 120 ± 9                       |
| SCFRP 10a 90° | 3 602 ± 182    | 3 537 ± 178                  | 180 ± 9                       |

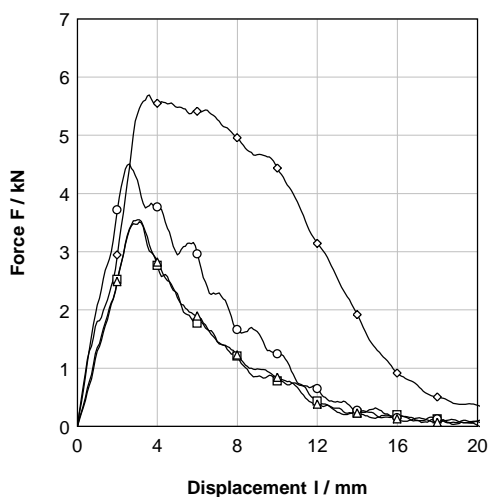
<sup>1)</sup> Determined between 2.000 and 52.825 mm pin displacement

the bearing force remains on a lower but nearly constant level ( $F_{mean}$ ), figure 3. Integrating the force vs. displacement data yields the energy ( $AE_{mean}$ ), which is absorbed by the composite.

In case of CFRP, damage is limited to a narrow area along the path of the pin. The failure mode is dominated by fibre breakage and fragmentation. Adding two top layers with steel fibres in parallel to the pin moving direction (SCFRP 10a 0°) has no beneficial influence on the bearing resistance. The coiling of the displaced steel fibres in front of the pin merely causes a continuous increase of the mean bearing force. By contrast, the bearing performance is significantly improved by adding two top layers with steel fibres vertically to the pin moving direction (SCFRP 10a 90°). Caused by the expulsion of the pin, the steel fibres delaminate from the CFRP core, are free to yield and to hinder the pin movement. Compared to CFRP, more extensive areas lateral to the track of the pin are degraded. As a consequence, the mean bearing force and thus the energy absorption rise 86 % compared to CFRP. Adding copper mesh on one side of the CFRP (CFRP + Cu) has no influence on the bearing performance.

#### 4.3 Dynamic penetration tests

Dynamic perforation tests are conducted according to DIN EN ISO 6603-2. A metallic indenter with a diameter of 20 mm and an impact energy of 193 J (corresponds with an impact velocity of 4.4 m/s) is dropped on composite plates. The plates are circular clamped with a free gauge length of



| Material   | $F_{max} / N$ | $l_p / mm$ <sup>1)</sup> | $AE_p / J$ <sup>2)</sup> |
|------------|---------------|--------------------------|--------------------------|
| CFRP       | 3 558 ± 336   | 5.76 ± 0.57              | 12.89 ± 0.70             |
| CFRP thick | 4 523 ± 91    | 6.95 ± 0.35              | 20.91 ± 0.86             |
| CFRP + Cu  | 3 598 ± 65    | 6.07 ± 0.60              | 13.56 ± 1.38             |
| SCFRP 20a  | 5 737 ± 46    | 12.55 ± 0.18             | 53.15 ± 0.93             |

<sup>1)</sup> Displacement, in which the force has fallen to half of its maximum

<sup>2)</sup> Energy, which is absorbed by the material at a displacement of  $l_p$

Figure 4: Results of dynamic perforation tension tests on multiaxial (hybrid) laminates

40 mm. The material response is characterised by the maximum force ( $F_{\max}$ ), the displacement, at which the force has fallen to half its maximum value ( $l_p$ ) and the absorbed energy ( $AE_p$ ). Figure 4 summarises the obtained results for the investigated laminates.

CFRP exhibits brittle failure behaviour. The failure mode is dominated by delamination and cracking. After exceeding a certain peak load, cracks grow free of energy absorption mostly at an angle of  $\pm 45^\circ$ , i.e. in direction of the majority of fibres. Increasing the thickness of the composite from 1.60 mm (CFRP) to 2.12 mm (CFRP thick) causes a slight increase of the maximum force. An additional copper mesh on the impacted side of the specimen (CFRP + Cu) has no significant influence on the penetration performance. By contrast, SCFRP 20a shows a distinctive ductile behaviour. On the rear side, bundles of steel fibres of the outer ply delaminate from the CFRP and yield. More pronounced deformations are only hindered by the fixture of the specimens. Compared to CFRP, the hybrid composite can bear larger deformation, while the load remains on a higher, slightly decreasing level. The energy absorption rises 312 % compared to CFRP and 154 % compared to the 2.12 mm thick CFRP (CFRP thick).

#### 4.4 Compression strength after impact tests

The low speed impact resistance of the multiaxial composites is characterised according to AITM 1-0010. Flat-faced rectangular specimens sized 150 by 100 mm are mounted to a plate with a clear window of 125 by 75 mm. The specimens are impacted by a metallic indenter with a diameter of 16 mm and distinguished impact energy. Repeated hits on the specimen by the indenter are prevented by using a suitable arresting device. Figure 5 shows the corresponding force-time-traces.

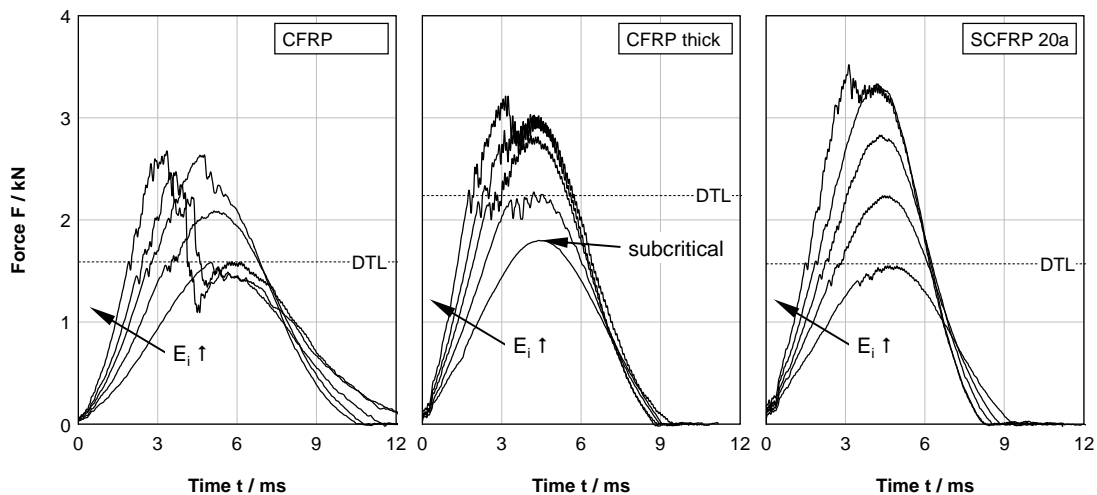


Figure 5: Force trace of impact tests on multiaxial (hybrid) laminates

After the impact, all samples were non-destructively tested by ultrasonics using the double-through-transmission technique with an auxiliary reflector to determine impact related damages. This technique allows ultrasonic testing of thin samples without front surface echo and back surface echo affecting the evaluating gate which had been set around the reflector echo. Thus, the distance between the rear side of the samples and the reflector was 5 mm to separate clearly back surface echo and reflector echo. The inspections were accomplished with an ultrasonic transducer providing a frequency of 5 MHz while having a focal length of 50 mm. The focal point was targeted on the auxiliary reflector. The step width was chosen to 0.2 mm. The threshold level for damage evaluation is set to 16 dB. Additionally, impact-induced variation of the magnetic volume fraction within the metastable austenitic steel fibre reinforced near-surface layers is captured. For this purpose, the area around the dent on front and back surface of the specimen is scanned with a magnetic inductive measuring device. The grid spacing is set to 5 mm. The measuring device quantifies deformation-induced phase transformations from paramagnetic austenite to ferromagnetic martensite. The test results are summarised in figure 6.

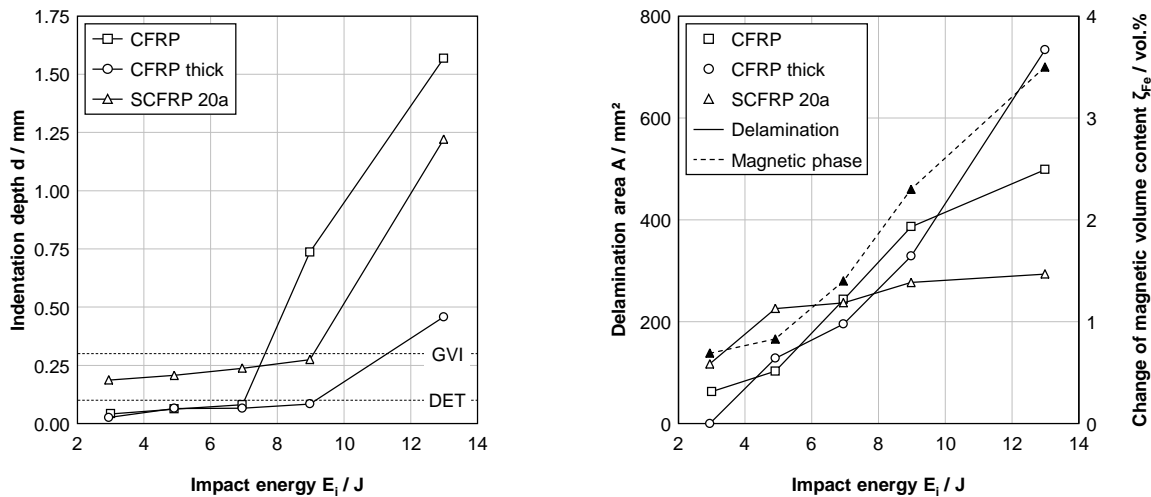


Figure 6: Results of the compression strength after impact tests on multiaxial (hybrid) laminates

The yielding of the metal fibres in the near surface layers of the laminate is additionally proved by the measurement of the magnetic volume fraction, figure 7. When plastically deformed, the metastable microstructure of the steel fibres changes from an austenitic to a martensitic structure. Consequently, after the impact, a pronounced increase of the magnetic signal at the area of the impact can be proved on the SCFRP surface. The change of the magnetic phase correlates to the location and intensity of the impact. The method provides a cost-efficient, non-destructive testing technology to detect and quantify damages in fibre hybrid composites by the help of phase transformations.

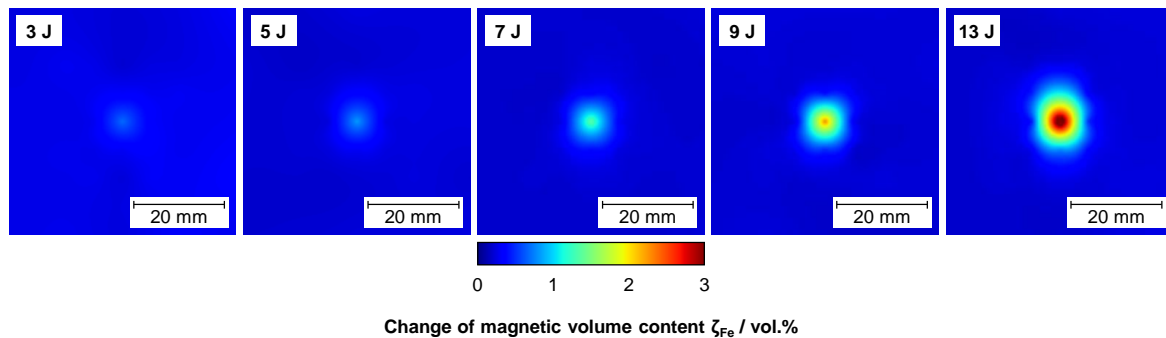


Figure 7: Magnetic volume content on the rear side of the impacted specimen

## 5 CONCLUSIONS

Several advantages of CFRP in comparison to aluminium alloys led to an increasing share of this composite in aviation industry. However, its comparatively poor electrical conductivity and limited damage tolerance causing additional weight, compromising today's CFRP lightweight potential. For this reason, efforts concentrate on modifying CFRP in order to guarantee the required electrical functionality and to improve its structure integrity. In this context, the present study analyses the potential of a hybrid composite consisting of endless carbon and stainless steel reinforcement fibres embedded in an epoxy resin.

Measurements on unidirectional reinforced (hybrid) composites prove significant enhancements of the electrical conductivity. Compared to conventional CFRP, the conductivity can be increased as a function of the steel fibre volume share and the specific electrical resistance of the incorporated metal fibres. However, despite the incorporation of highly ductile fibres, a pseudo-ductility in case of pure tensile load cannot be observed. The available ductility of the steel fibres is exploited only in very limited areas of the material. Consequently, the hybrid composites macroscopically exhibit a brittle tensile behaviour.

By contrast, in case of multiaxial laminates, hybrid composites with embedded steel fibres exhibit a distinguished post-failure behaviour. After failure of the carbon fibres, load is relocated to the steel fibres layers. The hybrid composite can bear further deformation on a lower level of load. Compared to CFRP, the total strain at failure can significantly be increased. This post-failure behaviour enables an improved structural performance. As a consequence, the pull-through strength of bolted joints is increased. Compared to CFRP, the hybrid material can bear larger deformation, while the maximum force remains on a higher level. Furthermore, the hybrid composites prove a higher resistance against bearing failure. Under bearing load, the hybrid material enables better energy absorption capabilities than conventional CFRP. Additionally, the penetration resistance of CFRP can be enhanced by incorporating steel fibres. The hybrid composite reveals complex failure modes. Different to CFRP, larger areas of the material can be addressed to absorb impact energy by plastic deformation of the steel fibres. In case of low velocity impacts, steel fibre reinforced top layers restrict the spread of impact-induced delamination. The corresponding yielding of the metal fibres can be visualised by measurement of the ferromagnetic volume share and correlated to the level of impact event. This technique provides a cost-efficient, non-destructive testing method to detect and quantify damages in metal-carbon fibre composites. However, with regard to a future application, the sensitivity to temperature changes and the reproducibility of this measurement technique have to be further analysed.

### ACKNOWLEDGEMENTS

The financial support of the German Research Foundation (DFG) within the projects BR 4262/2-1 and BA 4073/6-1 is gratefully acknowledged. Prepreg and resin film was kindly supplied by Cytec Engineered Materials GmbH (Östringen, Germany). Ultrasonic inspections were performed by the Institute for Plastic Technology Palatinate (University of Applied Sciences Kaiserslautern, Germany).

### REFERENCES

1. Breuer UP. Commercial Aircraft Composite Technology. Springer International Publishing, 2016:220-234.
2. Noll A, Friedrich K, Burkhart T, Breuer UP. Effective multifunctionality of poly (p-phenylene sulfide) nanocomposites filled with different amounts of carbon nanotubes, graphite and short carbon fibers. *Polym. Compos.* 2013;34(9):1405-1412.
3. Spitalsky Z, Tasis D, Papagelis K, Galiotis C. Carbon nanotube-polymer composites: Chemistry, processing, mechanical and electrical properties. *Prog. Polym. Sci.* 2010; 35(3):357-401.
4. Garg C, Mai YW. Failure mechanisms in toughened epoxy resins - A review. *Compos. Sci. Technol.* 1988; 31(3):179-223.
5. Medina Barron RM. Rubber toughened and nanoparticle reinforced epoxy composites. *IVW Schriftenreihe* 2009; 84.
6. Toho Tenax Europe GmbH. Product data sheet for Tenax<sup>®</sup> HTS filament yarn, Wuppertal 2014.
7. Hannemann B, Backe S, Schmeer S, Balle F, Breuer UP. Metal fiber incorporation in CFRP for improved electrical conductivity. *Mater. Sci. Eng. Technol.* 2016;47(11):1015-1023.